SUPPORTING INFORMATION

2,2',3,5',6-Pentachlorobiphenyl (PCB 95) is Atropselectively Metabolized to *Para* Hydroxylated Metabolites by Human Liver Microsomes

Eric Uwimana, Xueshu Li and Hans-Joachim Lehmler*

Interdisciplinary Graduate Program in Human Toxicology and Department of Occupational and Environmental Health, University of Iowa, Iowa City, IA 52242, United States.

Table of Content

Supplemental Experimental Section

Materials. 2,2',3,5',6-Pentachlorobiphenyl (PCB 95), 3-methoxy-2,2',4,5',6-pentachlorobiphenyl (methylated derivative of 3-103), 2,2',3,5',6-pentachlorobiphenyl-4-ol (4-95), 4'-methoxy-2,2',3,5',6-pentachlorobiphenyl (methylated derivative of 4'-95), 2,2',3,5',6-pentachlorobiphenyl-5-ol (5-95) and 4,5-dimethoxy-2,2',3,5',6-pentachlorobiphenyl (dimethylated derivative of 4,5-95) were synthesized as previously described.[1-3] 2,2',4,6'-Tetrachlorobiphenyl (PCB 51; internal standard); 2,3,4',5,6-pentachlorobiphenyl (PCB 117; recovery standard), 2,2',3,4,4',5,6,6'-octachlorobiphenyl (PCB 204; internal standard) and 2,3,3',4,5,5'-hexachlorobiphenyl-4'-ol (4'-159; recovery standard) were purchased from AccuStandard, Inc. (New Haven, CT, USA). Solutions of diazomethane in diethyl ether for the derivatization of hydroxylated PCB metabolites to methoxylated PCB derivatives were synthesized from *N*-methyl-*N*-nitroso-*p*-toluenesulfonamide (Diazald) using an Aldrich mini Diazald apparatus (Milwaukee, WI, USA).

β-Nicotinamide adenine dinucleotide 2'-phosphate reduced tetrasodium salt hydrate (NADPH) was purchased from Sigma-Aldrich (Milwaukee, WI, USA). Dimethyl sulfoxide (DMSO), sodium phosphate dibasic, sodium phosphate monobasic, magnesium chloride, tetrabutylammonium sulfite, sodium sulfite, and pesticide grade solvents were obtained from Fisher Scientific (Pittsburgh, PA, USA). Pooled human liver microsomes (catalog number H0620, pool of 50, mixed gender; lot numbers 0910398 or 1410013) and single-donor human liver microsomes (H1: catalog number H0531, lot number 0710185; H2, catalog number H0832, lot number 0910174; H3: catalog number H0779, lot number 0910130; H4: catalog number H0788, lot number 0910139; H5: catalog number H0444, lot number 0710042) were purchased from Xenotech (Lenexa, KS, USA).

PCB biotransformation assays. If not stated otherwise, incubations with human liver microsomes were performed in triplicate using an incubation system containing phosphate buffer (0.1 M, pH 7.4), magnesium chloride (3 mM), liver microsomes (0.1 mg/mL), and NADPH (1 mM) as described previously.[4, 5] These experimental conditions were optimized with regards to microsomal protein, NADPH and PCB 95 concentration. OH-PCB formation was linear for incubation times up to 15 min (single donor human liver microsomes) or 30 min (pooled human liver microsomes). Briefly, individual samples were preincubated for 5 min at 37°C in a shaking water bath. Racemic PCB 95 (50 µM in DMSO; ≤ 0.5% of the incubation volume) was added in a 2 mL incubation system and the mixtures were incubated for 5 to 15 min at 37°C. The reaction was stopped by adding ice-cold sodium hydroxide (2 mL, 0.5 M) to each sample. The incubation mixture was heated at 110 °C for 10 min to further denature the protein and solubilize the microsomes. Blank samples containing only phosphate buffer accompanied each experiment. In addition, control incubations without PCB were included for each microsomal preparation to check for background contamination with PCBs or their metabolites.

Extraction of PCBs and metabolites. PCB 95 and its hydroxylated metabolites were simultaneously extracted from the incubation mixture.[4, 5] Briefly, samples were spiked with surrogate recovery standards PCB 117 (200 ng) and 4'-159 (68.5 ng). Hydrochloric acid (6 M, 1 mL) was added, followed by 2-propanol (5 mL). The samples were extracted with hexane-MTBE (1:1 v/v, 5 mL) and re-extracted with hexane (3 mL). The combined organic layers were washed with an aqueous potassium chloride solution (1%, 4 mL). The organic phase was transferred to a new vial, and the KCl mixture was re-extracted with hexane (3 mL). The combined organic layers were evaporated to dryness under a gentle stream of nitrogen. The samples were reconstituted with hexane (1 mL), derivatized with diazomethane in diethyl ether

(0.5 mL) for approximately 16 h at 4 °C,[6] and underwent sulfur and sulfuric acid clean-up steps prior to gas chromatographic analysis.[7, 8]

Identification of PCB metabolites. Gas chromatography with time-of-flight mass spectrometry was used to identify the hydroxylated PCB metabolites (as the corresponding methylated derivatives) formed in incubations with pooled human liver microsomes. Incubations were performed as described above using the following experimental conditions to obtain high metabolite levels: 50 µM PCB 95; 90 minute incubation at 37 ºC with 0.3 mg/mL microsomal protein and 1 mM NADPH. Metabolites were extracted and derivatized as described above, and samples were analyzed on a Waters GCT Premier gas chromatograph (Waters Corporation, Milford, MA, USA) combined with a time-of-flight mass spectrometer in the High Resolution Mass Spectrometry Facility of the University of Iowa (Iowa City, IA, USA). Analytes were separated on a DB-5ms column (30 m × 250 µm × 0.25 µm film thickness; Agilent, Santa Clara, CA, USA). The oven temperature was held at 150 °C for 1 min, then ramped at a rate of 30 °C/min to a final temperature of 240 °C, and held for 15 minutes at 240 °C. The injector was operated in the splitless mode at a temperature of 280 °C. The helium flow rate was 1.5 ml/min. The source temperature was at 250°C, and a mass range of *m/z* 50 to 650 was collected.

Samples were analyzed with and without continuously introducing heptacosafluorotributylamine as internal standard (lock mass) to determine the accurate mass of $[M]^+$ and obtain mass spectra of the metabolites, respectively. The average relative retention times (RRT) (n=3) of the metabolites, calculated relative to PCB 51 as internal standard, were within 0.5% of the RRT of the respective authentic standard.[9] RRTs of M_1-95, M_2-95 and M_3-95 in individual samples were within 0.5% of the average RRT of the respective metabolite (n=3). All experimental accurate mass determinations were within 0.005 Da of the theoretical mass of

$[M]^+$. The isotope pattern of $[M]^+$ matched the theoretical abundance ratios of pentachlorinated biphenyl derivatives within a 20 % error. Representative gas chromatograms and mass spectra of the metabolites as well as corresponding authentic standards recorded without heptacosafluorotributylamine are shown in Figures S1-S14.

Quantification of metabolite levels. Sample extracts were analyzed on an Agilent 7890A gas chromatograph with a ^{63}Ni-micro electron capture detector (μECD) and a SPB-1 capillary column (60 m × 250 μm × 0.25 μm film thickness; Supelco, St Louis, MO, USA) as reported earlier.[10] Concentrations of hydroxylated PCB 95 metabolites (as methylated derivatives) were either determined following a published procedure[4, 5] using authentic standard or expressed as relative levels (*i.e.*, area of the metabolite relative to the area of the internal standard). PCB 204 was added as internal standard (volume corrector) prior to GC analysis for the quantification of PCB 95 metabolites based on their relative response factors as described previously.[4, 11] Since authentic standards of M_1-95, M_2-95 and M_3-95 were not available, relative metabolite levels and formation rates were expressed as area of the metabolite relative to the area of the internal standard (PCB 204). The average RRTs of the metabolites, calculated relative to PCB 204, were within 0.5% of the RRT for the respective standard or, for unknown metabolites, the RRT in individual samples were within 0.5% of the average RRT of the respective metabolite.[9]

Enantioselective gas chromatographic analyses. Enantioselective analyses were performed on extracts from long-term incubations (*i.e.*, 50 μM PCB 95, 120 minutes, 37 ºC, 0.5 mg/mL protein, and 0.5 mM NADPH) to determine which PCB 95 atropisomer is preferentially metabolized. In addition, 15 min incubations were carried using the optimized conditions described above (metabolite levels in the 5 min incubations did not allow a robust determination

of enantiomeric fractions; also see Table S6). Samples were analyzed using an Agilent 6890 gas chromatograph equipped with a ^{63}Ni-μECD detector and Chiral-Dex B-DM (BDM) (30 m × 250 μm × 0.12 μm film thickness, Supelco; St Louis, MO, USA) capillary column. The oven temperature was as follows: initial temperature was 50 °C held for 1 min, ramped at 10 °C/min to 139 °C and held for 520 min, the temperature was then ramped at 10 °C/min to the final temperature of 200 °C and held for 20 min. The helium flow was 3 mL/min. EF values were calculated by the drop valley method[12] as EF = Area E_1/(Area E_1 + Area E_2), were Area E_1 and Area E_2 denote the peak area of the first and second eluting atropisomer.

Quality assurance/quality control. The response of the electron capture detector was linear ($R^2 \geq 0.998$) for all analytes within the concentration range encountered in this study. The limits of detection (LOD) of the PCB 95 metabolites were calculated from blank buffer samples as LOD = mean blanks +k* Standard deviation blanks, (k is the student's t value for a degree of freedom of n-1=8 at the 99% confidence level). The LODs were 0.18, 0.18, 0.70, 0.24 and 0.05 ng for 3-103, 5-95, 4'-95, 4-95 and 4,5-95, respectively.[4, 5] Relative limits of detection for M_1-95, M_2-95 and M_3-95, expressed as relative peak area × 10^2, were 0.56, 0.01 and 0.05, respectively. Background levels for 3-103, 5-95, 4'-95, 4-95 and 4,5-95 in control (DMSO) incubations (n=8) were 0.06, 0.07, 0.17, 0.20 and 0.04 ng/mL, respectively. Background levels for M_1-95, M_2-95 and M_3-95 expressed as relative peak area/mL × 10^2, were 0.01, 0.01 and 0.2, respectively. The recoveries of PCB 117 and 4'-159 were 96 ± 14% (range: 49 to 143) and 107 ± 9% (range: 83 to 128), respectively. Levels of PCB and its metabolites were not adjusted for recovery to facilitate a comparison with earlier studies.[11] The resolution[4] of the atropisomers of PCB 95 and 4'-95 on the BDM column was 0.91 and 1.53, respectively. The EF values of the racemic standards of PCB 95 and 4'-95 were 0.50 ± 0.01 (n=5) and 0.48 ± 0.01 (n=4), respectively.

Table S1. Levels of OH-PCB 95 metabolites (ng/mg microsomal protein) in incubations with different human liver microsome (HLM) preparations. Data are expressed as mean ± SD, n = 3.

Incubation time	HLM Preparation	3-103	5-95	4'-95	4-95	4,5-95	Conversion[a]
5 min[b]	pHLM[c]	3.4 ± 0.1	1.9 ± 0.2	31 ± 2	3.8 ± 2.4	ND	0.02
	H1	5.7 ± 0.4	1.4 ± 0.1	45 ± 1	8.0 ± 0.2	ND	0.04
	H2	4.6 ± 0.2	2.3 ± 0.3	42 ± 2	9.0 ± 0.8	ND	0.04
	H3	4.9 ± 0.5	2.1 ± 0.1	39 ± 1	10.7 ± 1.7	ND	0.03
	H4	4.0 ± 0.2	3.1 ± 0.1	31 ± 1	5.7 ± 0.1	ND	0.03
	H5	5.7 ± 0.6	3.0 ± 0.4	53 ± 5	12.2 ± 1.1	ND	0.05
15 min[b]	pHLM[c]	10 ± 0.4	7 ± 0.5	93 ± 4	18 ± 0.7	ND	0.08
	H1	16 ± 0.2	4 ± 0.2	127 ± 3	16 ± 12	ND	0.10
	H2	15 ± 1.0	7 ± 0.3	130 ± 9	27 ± 1.8	1.8 ± 0.4	0.11
	H3	14 ± 0.2	6 ± 0.5	110 ± 2	26 ± 1.3	0.5 ± 0.1	0.10
	H4	11 ± 0.6	8 ± 0.1	85 ± 5	15 ± 0.6	0.4 ± 0.1	0.07
	H5	15 ± 0.5	10 ± 0.5	146 ± 5	34 ± 0.9	0.9 ± 0.1	0.13
120 min[d]	pHLM[e]	4.3 ± 0.5	4.0 ± 0.3	23 ± 2	3.9 ± 0.5	0.4 ± 0.1	1.1
	H1	26.7 ± 1.4	3.4 ± 0.2	112 ± 7	14.8 ± 0.4	2.5 ± 0.1	4.9
	H2	11.9 ± 0.8	3.6 ± 0.1	42 ± 2	7.0 ± 0.3	0.8 ± 0.1	2.0
	H3	4.2 ±0.1	6.7 ± 0.4	24 ± 1	3.8 ± 0.1	0.4 ± 0.1	1.2
	H4	2.3 ± 0.3	2.6 ± 0.2	14 ± 2	2.1 ± 0.2	0.2 ± 0.1	0.6
	H5	3.6 ± 0.1	4.5 ± 0.1	21 ± 1	3.4 ± 0.1	0.3 ± 0.1	1.0

[a] Percent of ΣOH-PCB of the total racemic PCB 95 added to each incubation.

[b] Incubation conditions: 50 μM PCB 95, 5 or 15 minute incubation at 37 ºC; 0.1 mg/mL microsomal protein; and 1 mM NADPH. These experimental conditions were optimized with regards to NADPH and PCB concentration, and the formation of all primary metabolites was linear with regards to incubation time and microsomal protein concentration.
[c] Lot number 1410013.
[d] Incubation conditions: 5 μM PCB 95; 120 minute incubation at 37 ºC; 0.5 mg/mL microsomal protein; and 0.5 mM NADPH.
[e] Lot number 0910398.
ND, not detected

Table S2. Relative rate of PCB 95 metabolite formation (relative peak area/nmol P450/min × 10^2) by different human liver microsome (HLM) preparations. Data are expressed as mean ± SD, n = 3.[a,b]

HLM Preparation[c]	3-103	M_1-95	M_2-95	5-95	4'-95	4-95
pHLM[d]	3.9 ± 0.1	0.5 ± 0.1	0.2 ± 0.1	0.7 ± 0.1	8.8 ± 0.4	0.9 ± 0.5
H1	4.7 ± 0.3	0.8 ± 0.1	0.3 ± 0.1	0.4 ± 0.1	9.6 ± 0.3	1.4 ± 0.1
H2	6.5 ± 0.2	0.5 ± 0.1	0.2 ± 0.1	1.0 ± 0.1	15.0 ± 0.8	2.8 ± 0.2
H3	6.5 ± 0.7	0.9 ± 0.1	0.5 ± 0.1	1.0 ± 0.1	13.8 ± 0.5	3.0 ± 0.5
H4	3.2 ± 0.2	0.4 ± 0.1	0.3 ± 0.1	0.8 ± 0.1	6.2 ± 0.2	0.9 ± 0.1
H5	8.1 ± 0.8	1.0 ± 0.1	0.4 ± 0.1	1.4 ± 0.2	18.8 ± 1.7	3.5 ± 0.3

[a] Microsomal metabolism studies were performed using the following incubation conditions: 50 μM PCB 95; 5 minute incubation at 37 ºC; 0.1 mg/mL microsomal protein; and 1 mM NADPH.
[b] Relative rates of metabolism were determined as described previously using total cytochrome P450 levels provided by Xenotech (Lenexa, KS, USA).[13, 14]
[c] See experimental section above for additional details regarding the human liver microsomes.
[d] Lot number 1410013.

Table S3. Relative rate of PCB 95 metabolite formation (relative peak area/mg microsomal protein/min × 10^2) by different human liver microsome (HLM) preparations. Data are expressed as mean ± SD, n = 3.[a,b]

HLM Preparation[c]	3-103	M_1-95	M_2-95	5-95	4'-95	4-95
pHLM[d]	2.2 ± 0.1	0.3 ± 0.1	0.1 ± 0.1	0.4 ± 0.1	5.1 ± 0.3	0.5 ± 0.3
H1	3.3 ± 0.2	0.4 ± 0.1	0.1 ± 0.1	0.3 ± 0.1	6.7 ± 0.2	1.0 ± 0.1
H2	2.9 ± 0.1	0.4 ± 0.1	0.1 ± 0.1	0.5 ± 0.1	6.5 ± 0.3	1.2 ± 0.1
H3	3.1 ± 0.3	0.4 ± 0.1	0.2 ± 0.1	0.5 ± 0.1	6.6 ± 0.2	1.4 ± 0.2
H4	2.5 ± 0.1	0.3 ± 0.1	0.2 ± 0.1	0.6 ± 0.1	4.9 ± 0.1	0.7 ± 0.1
H5	3.6 ± 0.4	0.4 ± 0.1	0.2 ± 0.1	0.6 ± 0.1	8.4 ± 0.8	1.6 ± 0.1

[a] Microsomal metabolism studies were performed using the following incubation conditions: 50 μM PCB 95; 5 minute incubation at 37 ºC; 0.1 mg/mL microsomal protein; and 1 mM NADPH.
[b] Relative rates of metabolism were determined as described previously.[13, 14]
[c] See experimental section above for additional details regarding the human liver microsomes.
[d] Lot number 1410013.

Table S4. Rate of PCB 95 metabolite formation (ng OH-PCB/nmol P450/min) by different human liver microsome (HLM) preparations. Data are expressed as mean ± SD, n = 3.[a,b]

HLM Preparation[c]	3-103	5-95	4'-95	4-95
pHLM[d]	1.2 ± 0.1	0.7 ± 0.1	10.8 ± 0.5	1.3 ± 0.8
H1	1.6 ± 0.1	0.4 ± 0.1	12.9 ± 0.3	2.3 ± 0.1
H2	2.1 ± 0.1	1.0 ± 0.1	19.1 ± 1.0	4.1 ± 0.3
H3	2.1 ± 0.2	0.9 ± 0.1	16.1 ± 0.6	4.5 ± 0.7
H4	1.0 ± 0.1	0.8 ± 0.1	8.0 ± 0.2	1.5 ± 0.1
H5	2.5 ± 0.3	1.4 ± 0.2	23.7 ± 2.2	5.5 ± 0.5

[a] Microsomal metabolism studies were performed using the following incubation conditions: 50 μM PCB 95; 5 minute incubation at 37 ºC; 0.1 mg/mL microsomal protein; and 1 mM NADPH.
[b] Rates of metabolism were calculated as described previously using total cytochrome P450 levels provided by Xenotech (Lenexa, KS, USA).[13, 14]
[c] See experimental section above for additional details regarding the human liver microsomes.
[d] Lot number 1410013.

Table S5. Rate of PCB 95 metabolite formation (ng OH-PCB/mg microsomal protein/min) by different human liver microsome (HLM) preparations. Data are expressed as mean ± SD, n = 3.[a,b]

HLM Preparation[c]	3-103	5-95	4'-95	4-95
pHLM[d]	0.7 ± 0.1	0.4 ± 0.1	6.3 ± 0.3	0.8 ± 0.5
H1	1.1 ± 0.1	0.3 ± 0.1	8.9 ± 0.2	1.6 ± 0.1
H2	0.9 ± 0.1	0.5 ± 0.1	8.3 ± 0.4	1.8 ± 0.2
H3	1.0 ± 0.1	0.4 ± 0.1	7.7 ± 0.3	2.1 ± 0.3
H4	0.8 ± 0.1	0.6 ± 0.1	6.3 ± 0.2	1.1 ± 0.1
H5	1.1 ± 0.1	0.6 ± 0.1	10.6 ± 1.0	2.4 ± 0.2

[a] Microsomal metabolism studies were performed using the following incubation conditions: 50 μM PCB 95; 5 minute incubation at 37 ºC; 0.1 mg/mL microsomal protein; and 1 mM NADPH.
[b] Rates of metabolism were calculated as described previously.[13, 14]
[c] See experimental section above for additional details regarding the human liver microsomes.
[d] Lot number 1410013.

Table S6: Enantiomeric fractions (EF) of PCB 95 and 4'-95 in incubations with human liver microsomes reveal the enantioselective formation of the second eluting 4'-95 atropisomer and, in a few cases, a depletion of the second eluting atropisomer of PCB 95. If not stated otherwise, data are expressed as mean ± SD, n = 3.

HLM Preparation[a]	Short term incubation (15 minutes)[b]		Long term incubation (120 minutes)[c]	
	EF PCB 95[d]	EF 4'-95[e]	EF PCB 95[d]	EF 4'-95[e]
Pooled	0.50 ± 0.01[f]	0.15 ± 0.01[f,*]	0.51 ± 0.01[g,h]	0.23 ± 0.02[g,h,*]
H1	0.50 ± 0.01	0.10 ± 0.01*	0.55 ± 0.01*	0.10 ± 0.01*
H2	0.50 ± 0.01	0.18 ± 0.01*	0.54 ± 0.01*	0.19 ± 0.01*
H3	0.50 ± 0.01	0.18 ± 0.01*	0.51 ± 0.01	0.23 ± 0.02*
H4	0.50 ± 0.01	0.11 ± 0.01[h,*]	0.50[i]	0.26[i]
H5	0.50 ± 0.01	0.21 ± 0.01*	0.51 ± 0.01	0.25 ± 0.01*

To allow a comparison with previously published data,[4] EF values were calculated by the drop valley method[12] using the following equation: EF = Area E_1/(Area E_1 + Area E_2), were Area E_1 and Area E_2 denote the peak area of the first and second eluting atropisomer. In the case of 4'-95, the second eluting atropisomer of 4'-95 (E_2-4'-95) co-eluted with the first eluting atropisomer of 4,5-95 (E_1-4,5-95) (Figure S17). Therefore, the apparent EF values of 4'-95 may slightly overestimate the extent of the atropisomeric enrichment of E_2-4'-95; however, this effect is small because of the low levels of 4,5-95 present in all microsomal incubations (*i.e.*, not detected to < 3% of the 4'-95 levels; Table S1). Additional discussion of the effect of the co-elution of E_2-4'-95 and E_1-4,5-95 on the EF values reported in this Table and illustrated in Figure 2 is provided in Figure S17 below. Please see the experimental section above for additional details regarding the enantioselective gas chromatographic analyses.

[a] See experimental section above for additional information.

[b] Incubation conditions: 50 μM PCB 95, 15 minute incubation at 37 ºC; 0.1 mg/mL microsomal protein; and 1 mM NADPH. These experimental conditions were optimized with regards to NADPH and PCB concentration, and the formation of all primary metabolites was linear with regards to incubation time and microsomal protein concentration.

[c] Incubation conditions: 5 μM PCB 95; 120 minute incubation at 37 ºC; 0.5 mg/mL microsomal protein; and 0.5 mM NADPH.

[d] Resolution of PCB 95 atropisomers = 0.91.[7]

[e] Resolution of 4'-95 atropisomers = 1.53.[7]

[f] Lot number 1410013.

[g] Lot number 0910398.

[h] n = 2.

[i] n = 1.

* Significantly different from the EF value of the respective racemic standard ($p < 0.05$, t-test).

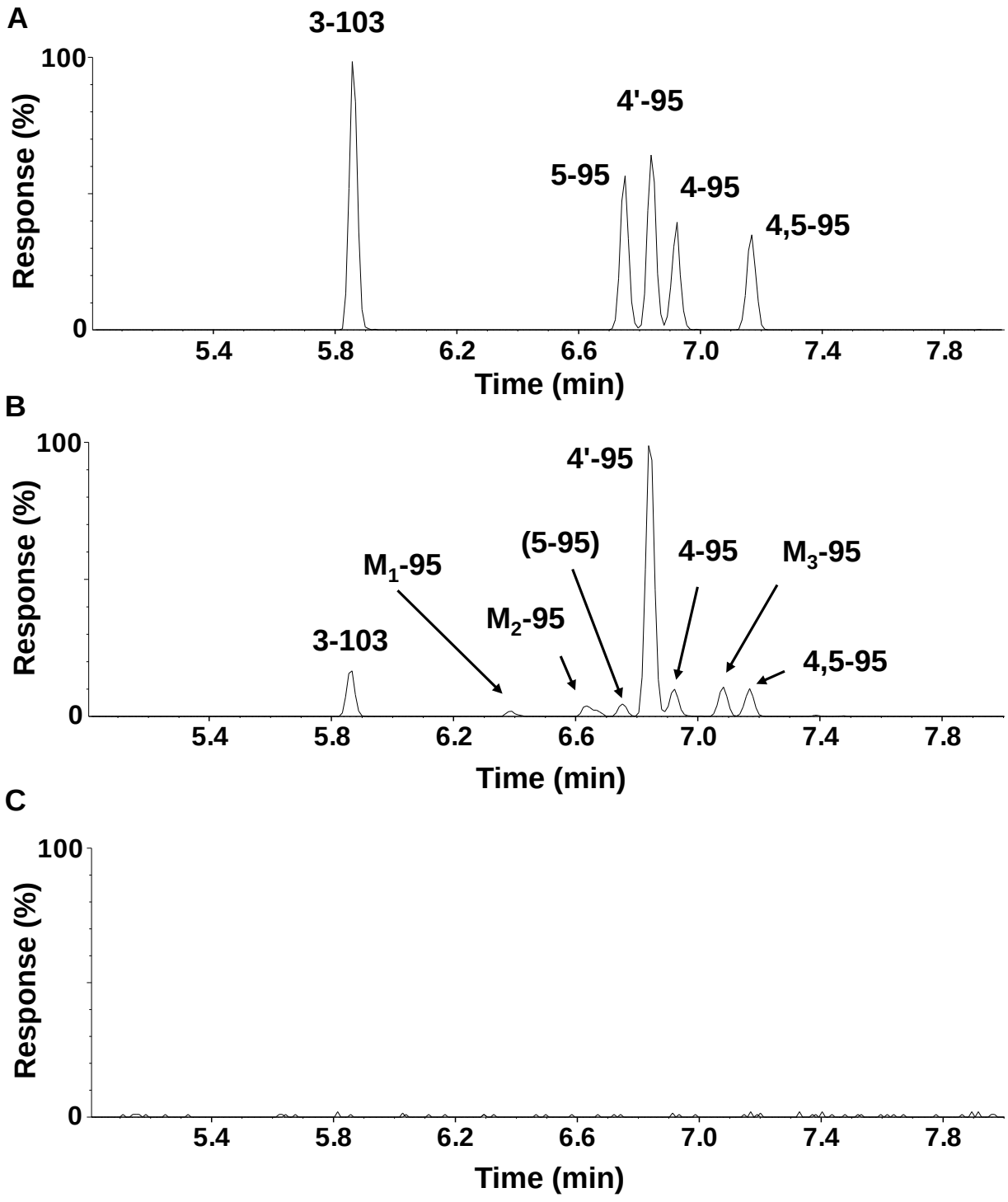

Figure S1. PCB 95 is metabolized to six monohydroxylated metabolites (*m/z* 355.9), including 3-103, M_1-95, M_2-95, 5-95, 4'-95 and 4-95, and two dihydroxylated metabolites (*m/z* 385.9), M_3-95 and 4,5-95. Gas chromatograms showing the (A) reference standard with five PCB 95

metabolites; (B) extract from incubations of PCB 95 with pooled human liver microsomes; and (C) solvent (DMSO) control incubation after derivatization with diazomethane showing the absence of PCB 95 metabolites. Peak heights in panels A and B are adjusted relative to the highest peak in the chromatogram. The blank chromatogram in panel C is expressed relative to the highest peak in panel B for comparison purposes. The mass spectra of the authentic standards are shown in Figure S2-S6. Mass spectra of the metabolites formed in a representative microsomal incubation with a detailed description of the criteria used for the identification of the metabolites are presented in Figures S7-S14. Incubation conditions were as follows: 50 μM PCB 95; 90 minute incubation at 37 ºC; 0.3 mg/mL microsomal protein; and 1 mM NADPH. Please see the experimental section above for additional details regarding the microsomal incubations and the GC-MS analyses.

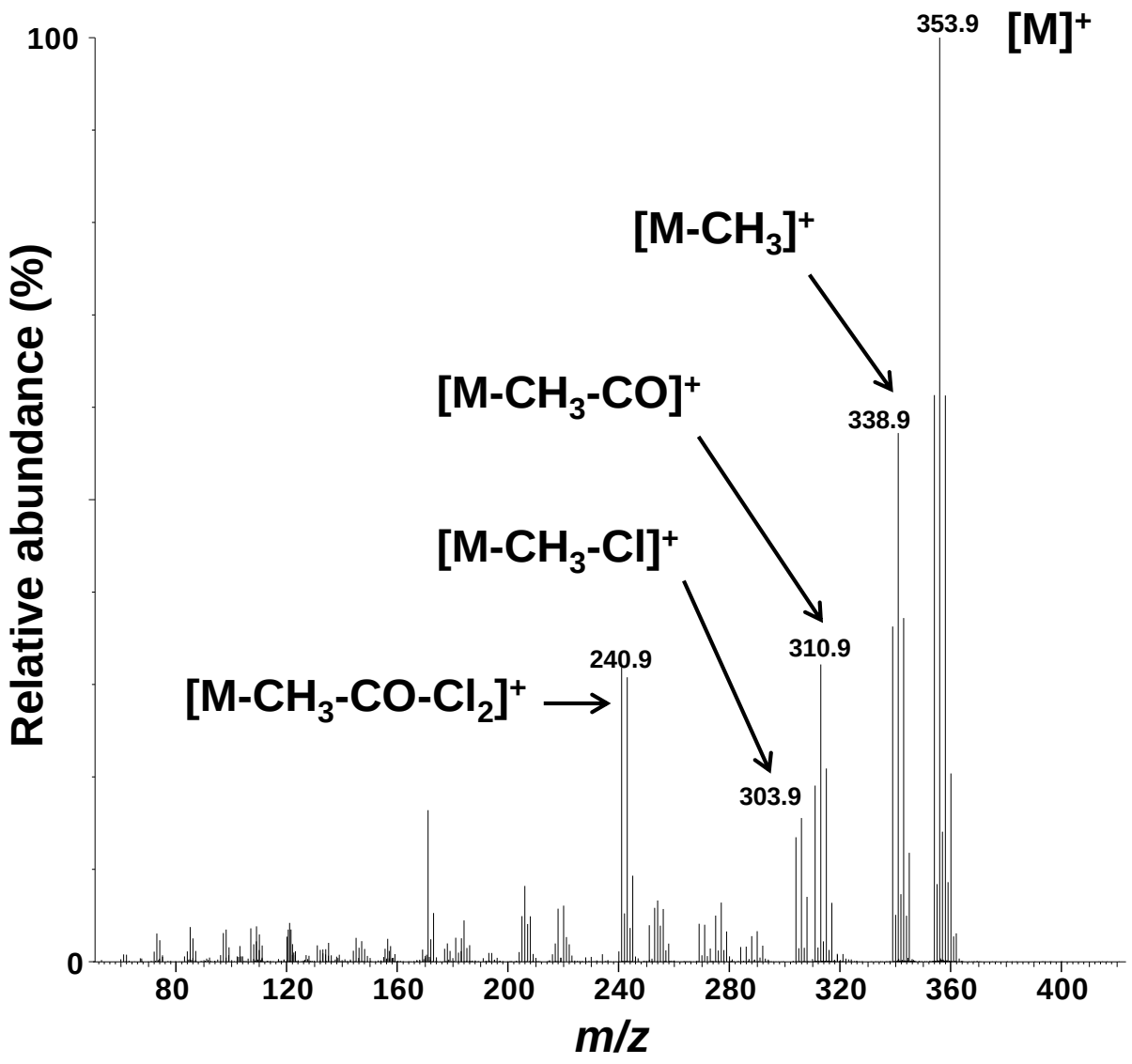

Figure S2. Mass spectrum of an authentic standard of 3-103 (RT 5.86 min; RRT 1.347). The accurate mass determination of the monoisotopic $[M]^+$ (*m/z* 353.8962 compared to *m/z* 353.8940, calculated for $C_{13}H_7O_1{}^{35}Cl_5$), the isotope pattern of the molecular ion (abundance ratio: 1:1.6:1:0.3 compared to predicted abundance ratio 1:1.6:1:0.3) and the fragmentation pattern are consistent with a monohydroxylated pentachlorobiphenyl (as the corresponding methylated derivative). The mass spectrum was recorded in the absence of the lock standard to improve the sensitivity, see the experimental section above for additional details.

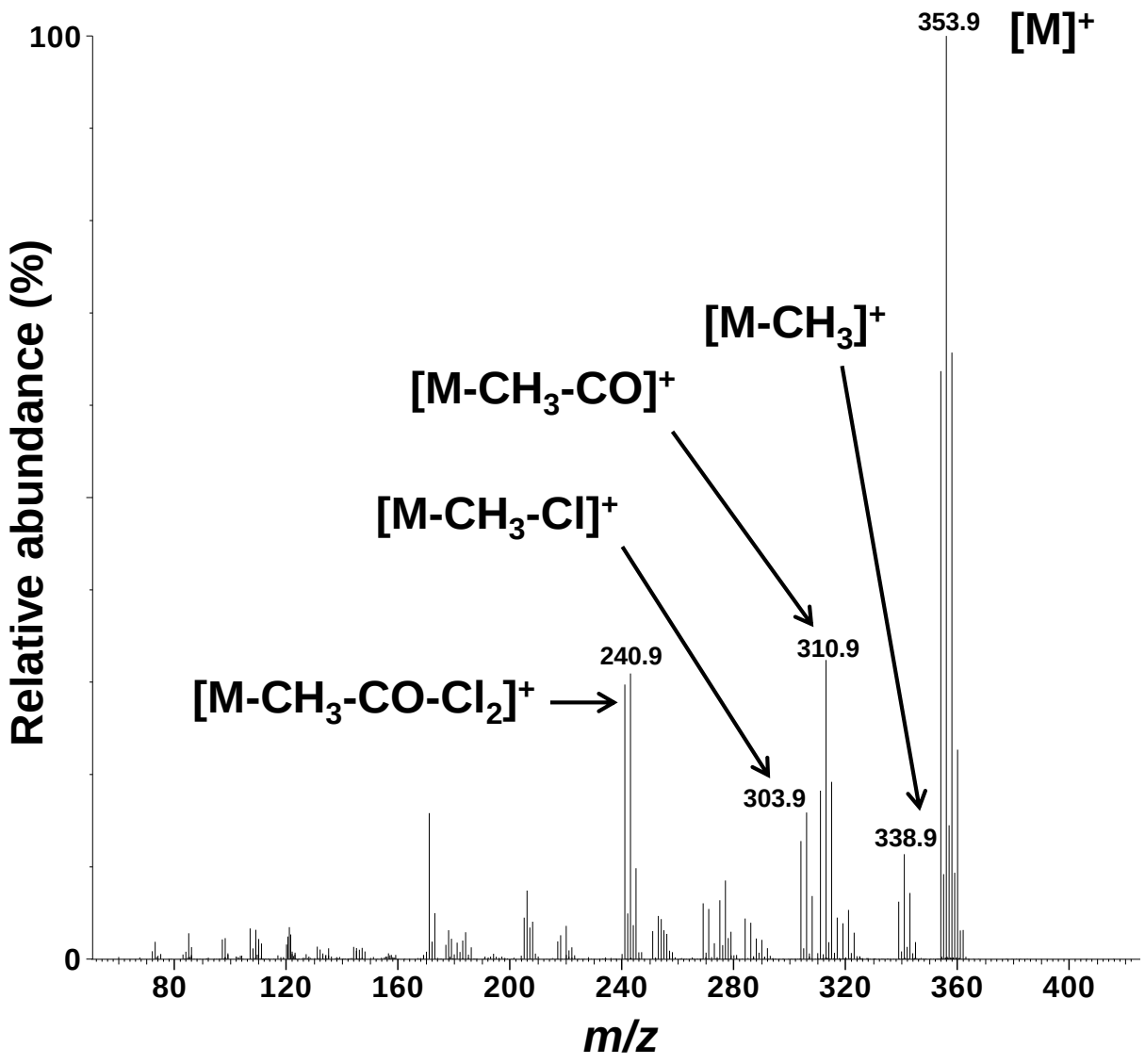

Figure S3. Mass spectrum of an authentic standard of 5-95 (RT 6.75 min; RRT 1.552). The accurate mass determination of the monoisotopic $[M]^+$ (*m/z* 353.8955 compared to *m/z* 353.8940, calculated for $C_{13}H_7O_1{}^{35}Cl_5$), the isotope pattern of the molecular ion (abundance ratio: 1:1.6:1:0.4 compared to predicted abundance ratio 1:1.6:1:0.3) and the fragmentation pattern are consistent with a monohydroxylated pentachlorobiphenyl (as the corresponding methylated derivative). The mass spectrum was recorded in the absence of the lock standard to improve the sensitivity, see the experimental section above for additional details.

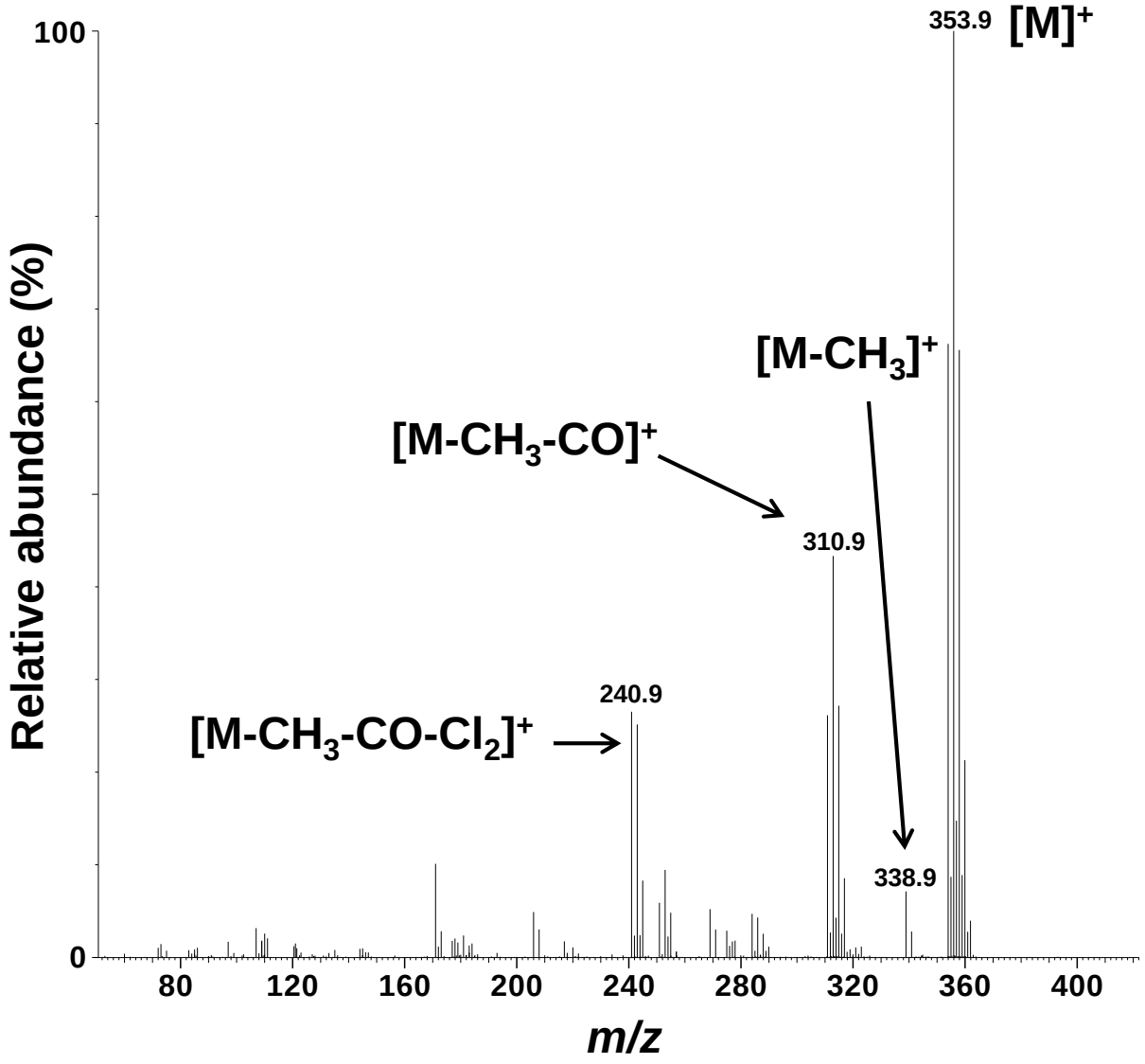

Figure S4. Mass spectrum of an authentic standard of 4'-95 (RT 6.84 min; RRT 1.572). The accurate mass determination of the monoisotopic $[M]^+$ (*m/z* 353.8958 compared to *m/z* 353.8940, calculated for $C_{13}H_7O_1{}^{35}Cl_5$), the isotope pattern of the molecular ion (abundance ratio: 1:1.5:1:0.3 compared to predicted abundance ratio 1:1.6:1:0.3) and the fragmentation pattern are consistent with a monohydroxylated pentachlorobiphenyl (as the corresponding methylated derivative). The mass spectrum was recorded in the absence of the lock standard to improve the sensitivity, see the experimental section above for additional details.

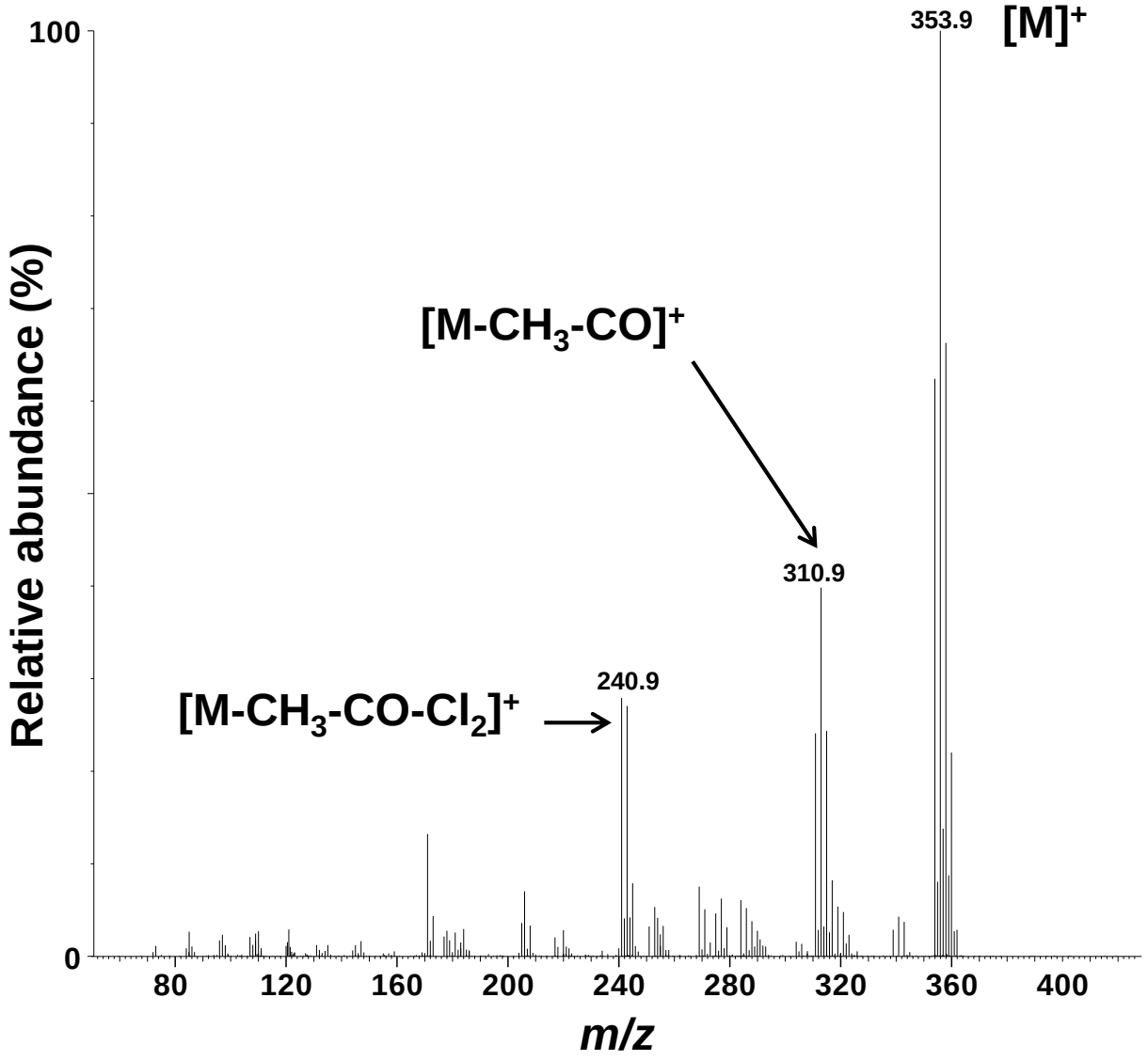

Figure S5. Mass spectrum of an authentic standard of 4-95 (RT 6.92 min; RRT 1.591). The accurate mass determination of the monoisotopic $[M]^+$ (*m/z* 353.8957 compared to *m/z* 353.8940, calculated for $C_{13}H_7O_1{}^{35}Cl_5$), the isotope pattern of the molecular ion (abundance ratio: 1:1.6:1.1:0.4 compared to predicted abundance ratio 1:1.6:1:0.3) and the fragmentation pattern are consistent with a monohydroxylated pentachlorobiphenyl (as the corresponding methylated derivative). The mass spectrum was recorded in the absence of the lock standard to improve the sensitivity, see the experimental section above for additional details.

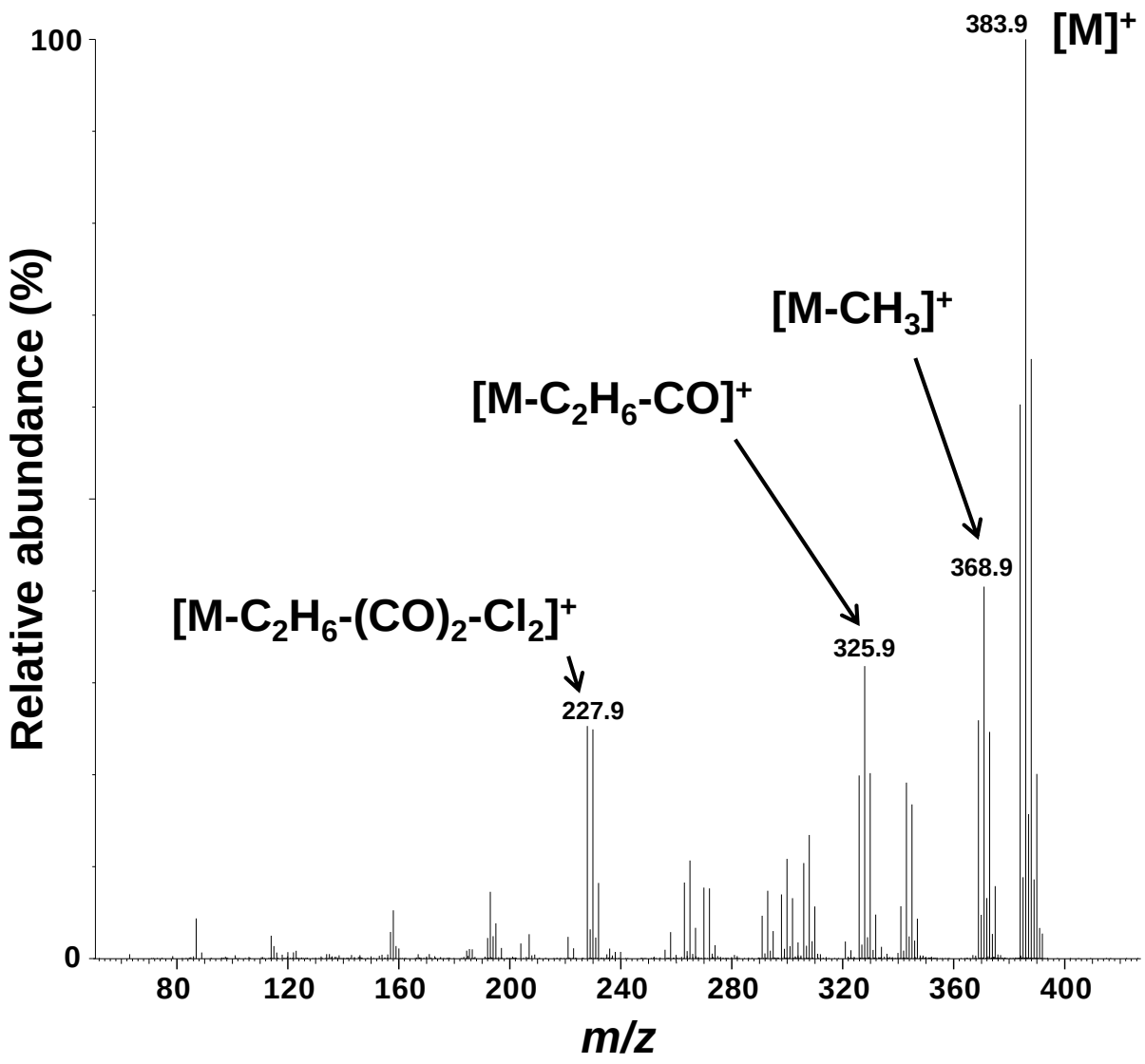

Figure S6. Mass spectrum of an authentic standard of 4,5-95 (RT 7.17 min; RRT 1.648). The accurate mass determination of the monoisotopic $[M]^+$ (*m/z* 383.9070 compared to *m/z* 383.9045, calculated for $C_{14}H_9O_2{}^{35}Cl_5$), the isotope pattern of the molecular ion (abundance ratio: 1:1.7:1.1:0.3 compared to predicted abundance ratio 1:1.6:1:0.3) and the fragmentation pattern are consistent with a dihydroxylated pentachlorobiphenyl (as the corresponding methylated derivative). The mass spectrum was recorded in the absence of the lock standard to improve the sensitivity, see the experimental section above for additional details.

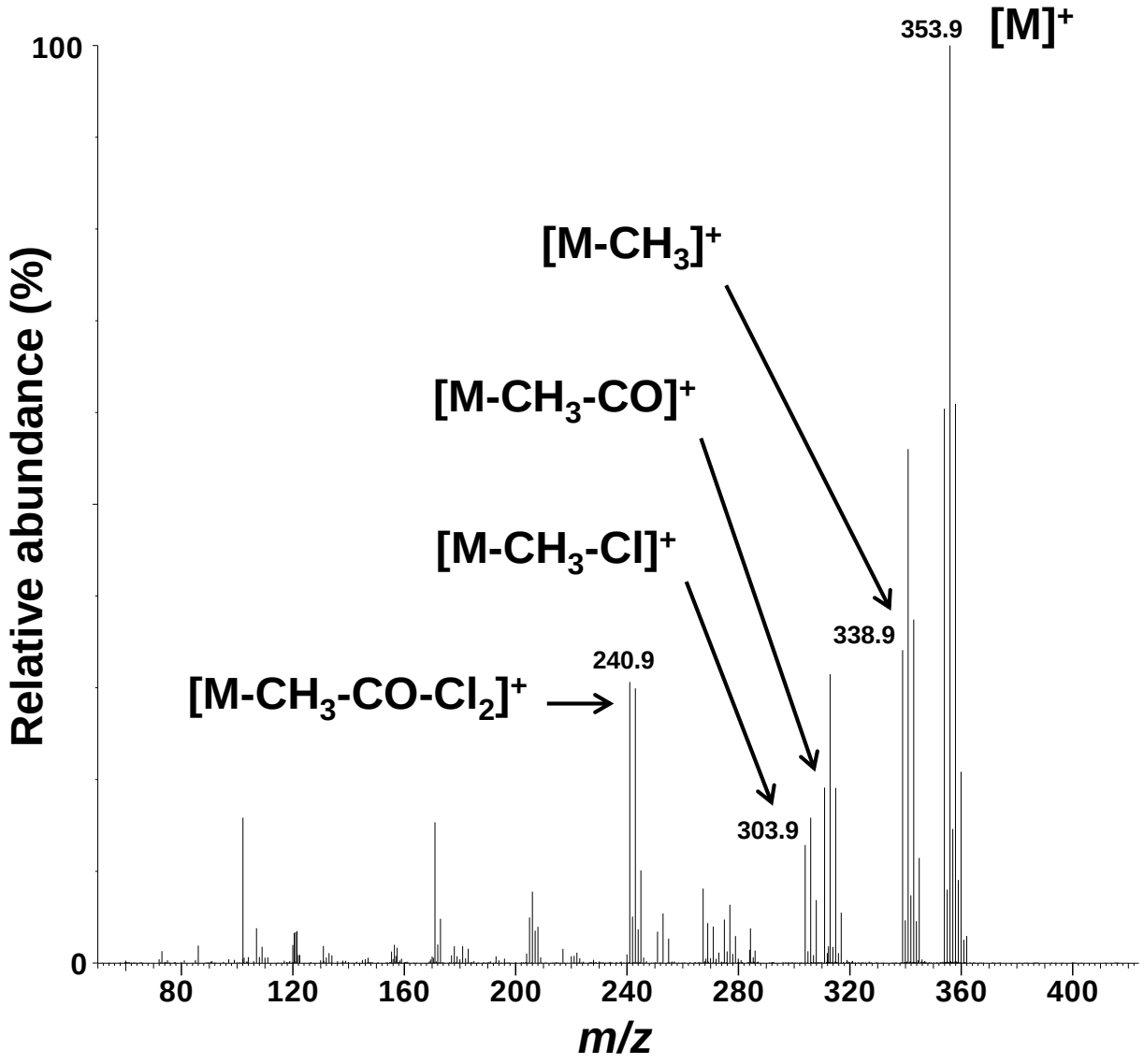

Figure S7. Mass spectrum of 3-103 (RT 5.87 min; RRT 1.346) formed in incubations of PCB 95 with pooled human liver microsomes. The accurate mass determination of the monoisotopic $[M]^+$ (*m/z* 353.8955 compared to *m/z* 353.8940, calculated for $C_{13}H_7O_1{}^{35}Cl_5$), the isotope pattern of the molecular ion (abundance ratio: 1:1.7:1:0.4 compared to predicted abundance ratio 1:1.6:1:0.3) and the fragmentation pattern are consistent with a monohydroxylated pentachlorobiphenyl (as the corresponding methylated derivative). The mass spectrum was recorded in the absence of the lock standard to improve the sensitivity, see the experimental section above for additional details.

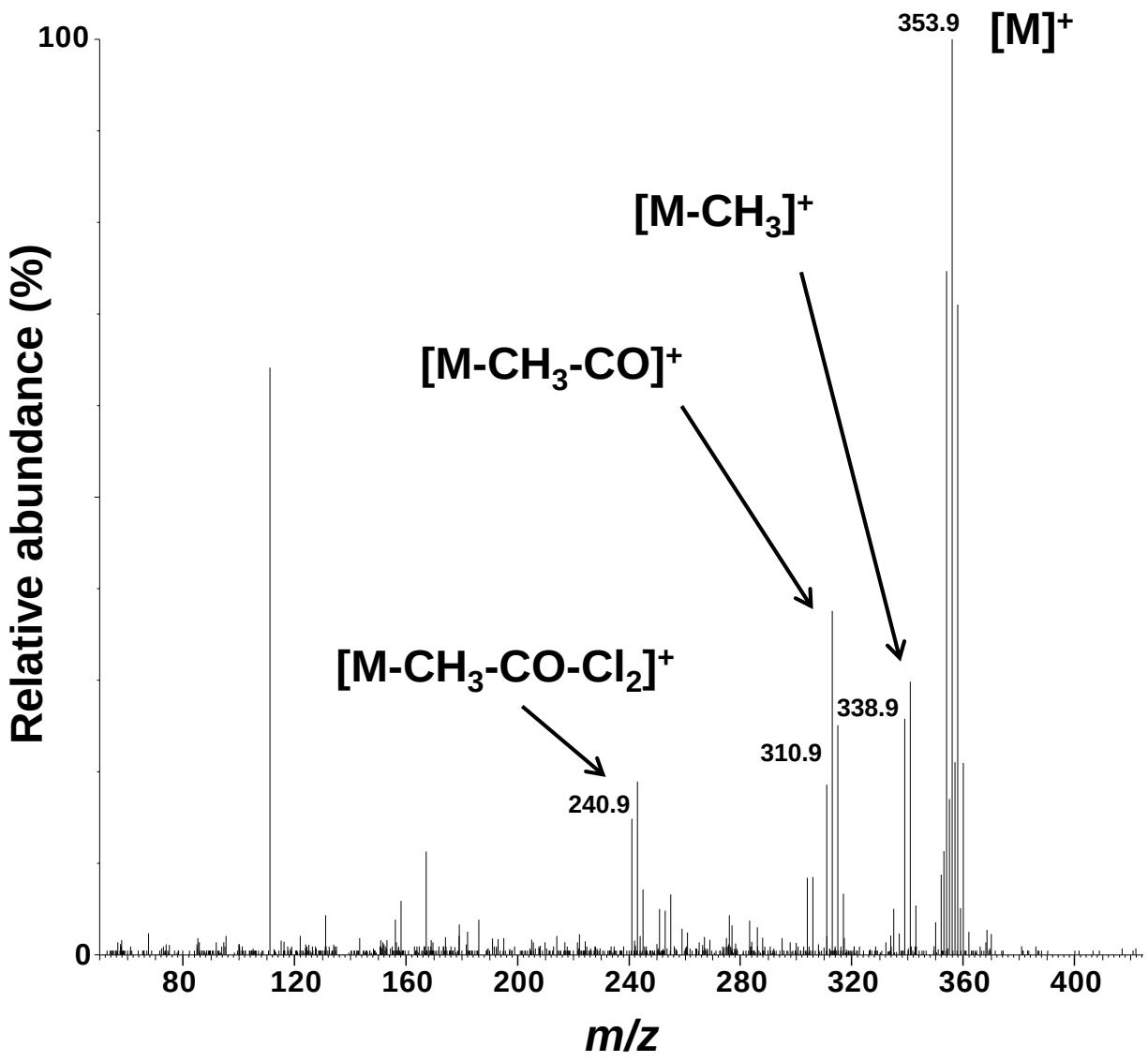

Figure S8. Mass spectrum of M_1-95 (RT 6.40 min; RRT 1.468), a peak tentatively identified as a monohydroxylated metabolite, formed in incubations of PCB 95 with pooled human liver microsomes. The mass spectrum was recorded in the absence of the lock standard to improve the sensitivity, see the experimental section above for additional details.

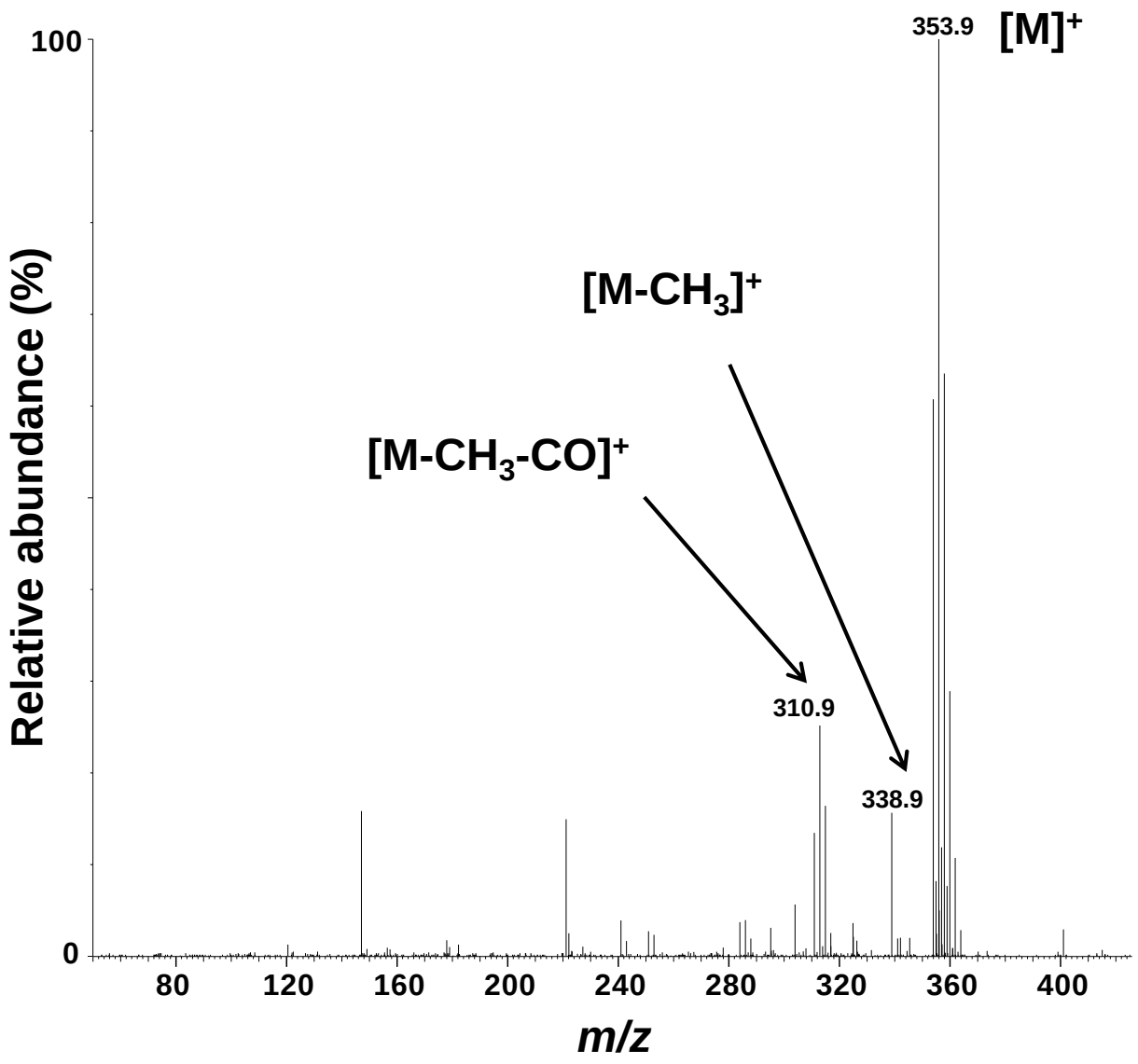

Figure S9. Mass spectrum of M_2-95 (RT 6.64 min; RRT 1.518), a peak tentatively identified as a monohydroxylated metabolite, formed in incubations of PCB 95 with pooled human liver microsomes. The accurate mass determination of the monoisotopic $[M]^+$ (*m/z* 353.8981 compared to *m/z* 353.8940, calculated for $C_{13}H_7O_1{}^{35}Cl_5$), and the isotope pattern of the molecular ion (abundance ratio: 1:1.6:1.1:0.5 compared to predicted abundance ratio 1:1.6:1:0.3) are consistent with a monohydroxylated pentachlorobiphenyl (as the corresponding methylated derivative). The mass spectrum was recorded in the absence of the lock standard to improve the sensitivity, see the experimental section above for additional details.

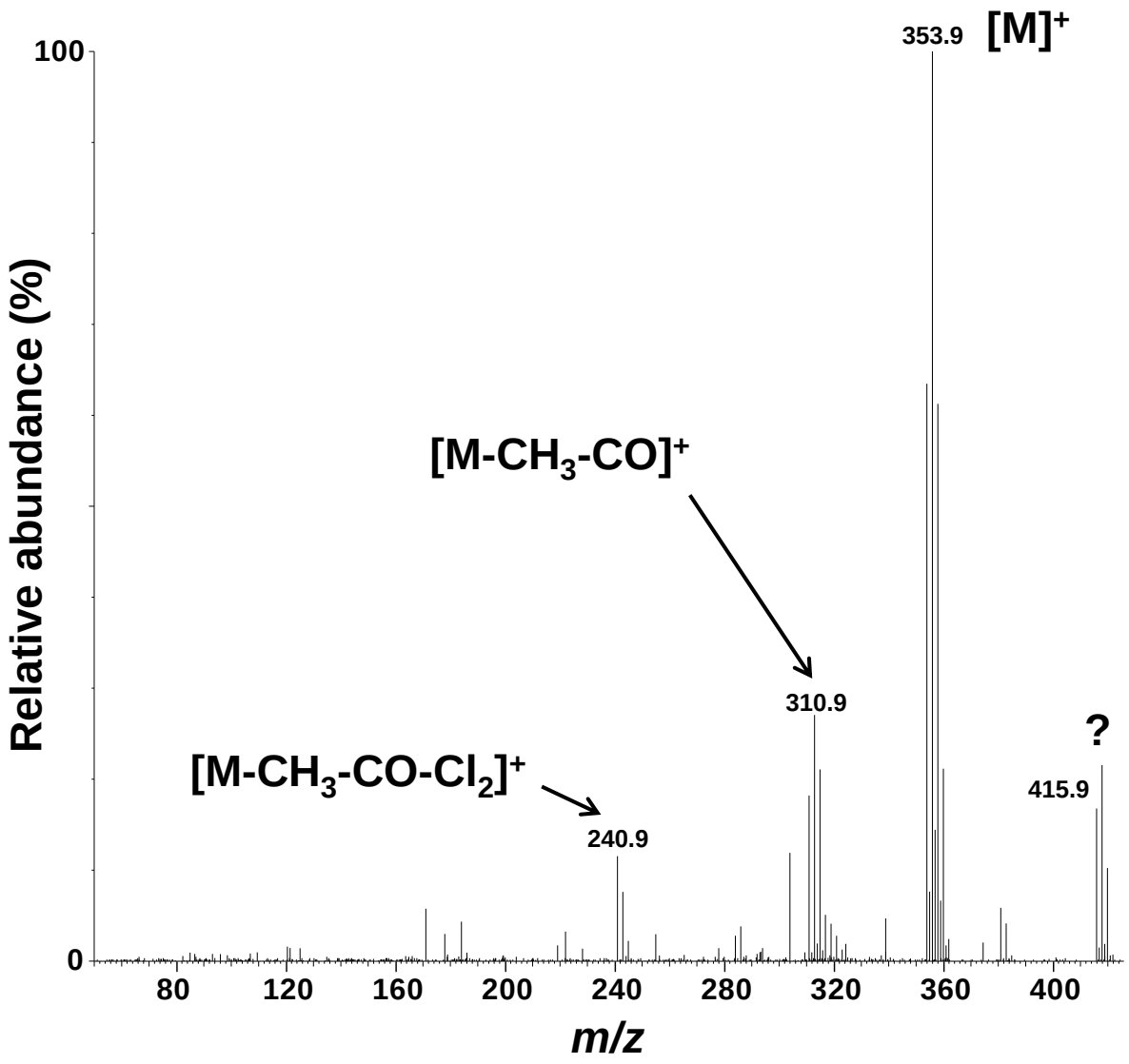

Figure S10. Mass spectrum of a minor metabolite tentatively identified as 5-95 (RT 6.75 min; RRT 1.548) formed in incubations of PCB 95 with pooled human liver microsomes. This metabolite was identified primarily based on its RRT (Figure S1). An unambiguous identification of 5-95 based on the mass spectral data is not possible due to the presence of an ion cluster around *m/z* = 415.9; however, this ion cluster is most likely due to a co-eluting impurity. The mass spectrum was recorded in the absence of the lock standard to improve the sensitivity, see the experimental section above for additional details.

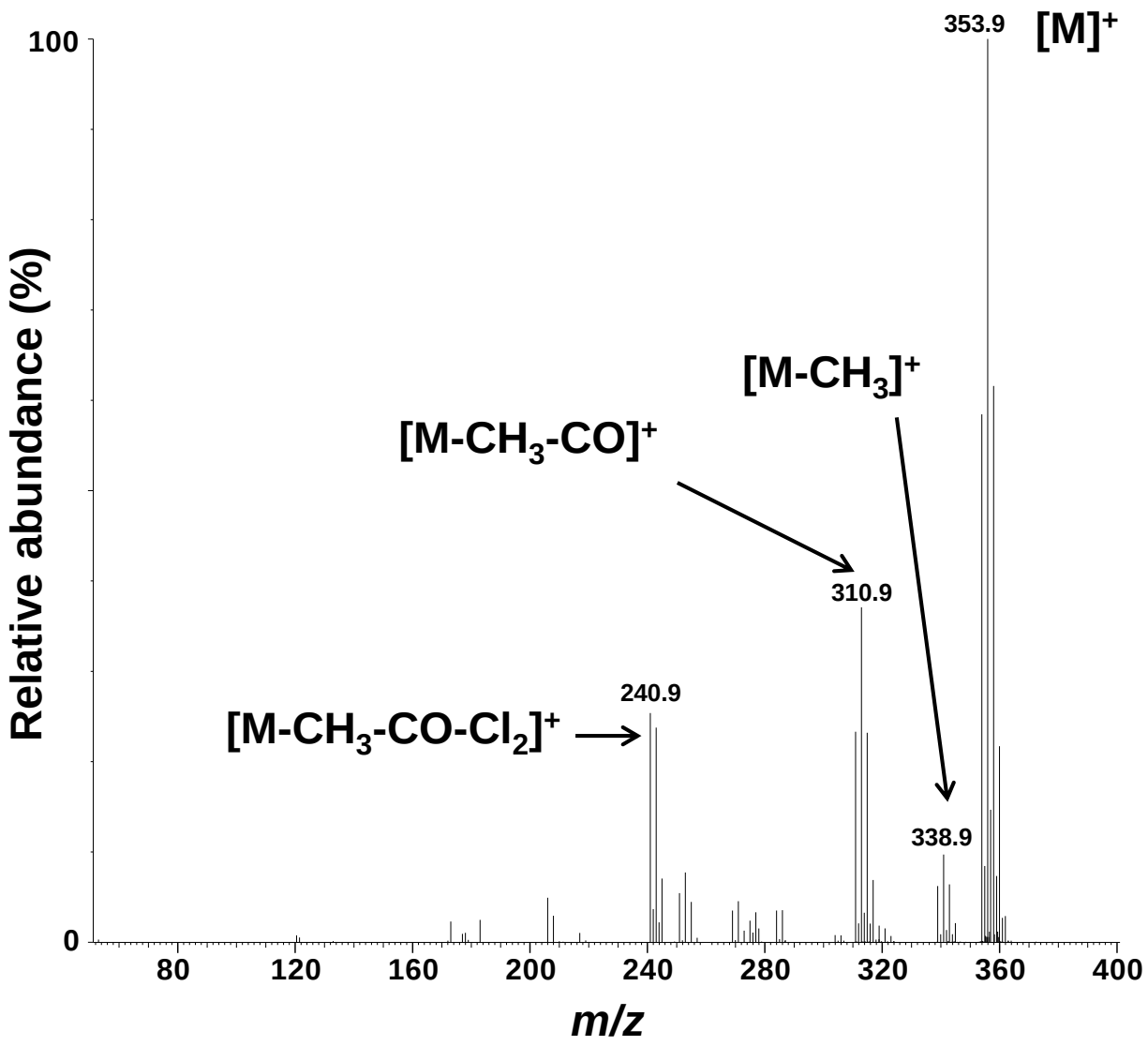

Figure S11. Mass spectrum of 4'-95 (RT 6.84 min; RRT 1.569) formed in incubations of PCB 95 with pooled human liver microsomes. The accurate mass determination of the monoisotopic $[M]^+$ (*m/z* 353.8978 compared to *m/z* 353.8940, calculated for $C_{13}H_7O_1{}^{35}Cl_5$), the isotope pattern of the molecular ion (abundance ratio: 1:1.6:1:0.3 compared to predicted abundance ratio 1:1.6:1:0.3) and the fragmentation pattern are consistent with a monohydroxylated pentachlorobiphenyl (as the corresponding methylated derivative). The mass spectrum was recorded in the absence of the lock standard to improve the sensitivity, see the experimental section above for additional details.

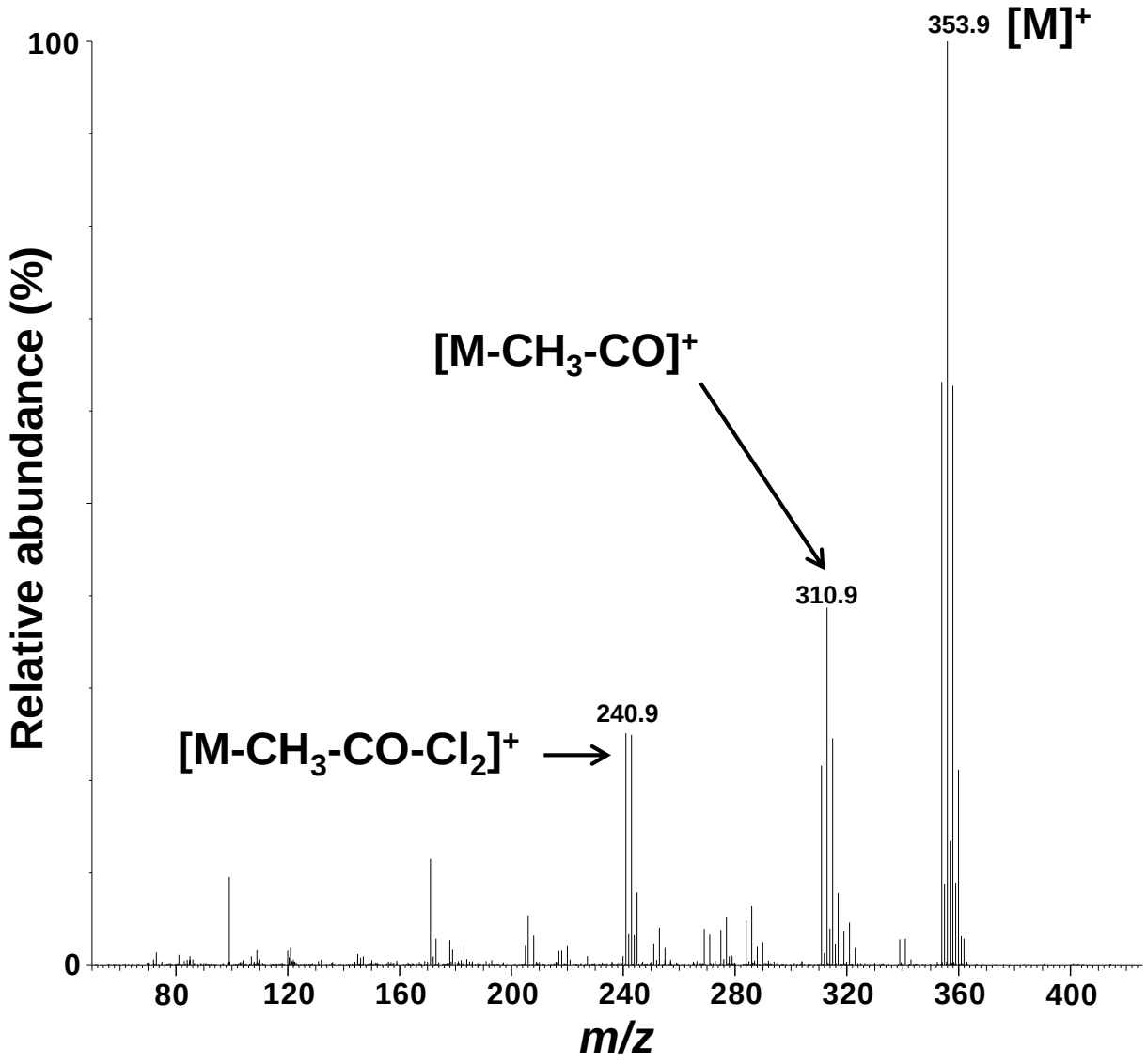

Figure S12. Mass spectrum of 4-95 (RT 6.92 min; RRT 1.587) formed in incubations of PCB 95 with pooled human liver microsomes. The accurate mass determination of the monoisotopic $[M]^+$ (*m/z* 353.8971 compared to *m/z* 353.8940, calculated for $C_{13}H_7O_1{}^{35}Cl_5$), the isotope pattern of the molecular ion (abundance ratio: 1:1.6:1:0.3 compared to predicted abundance ratio 1:1.6:1:0.3) and the fragmentation pattern are consistent with a monohydroxylated pentachlorobiphenyl (as the corresponding methylated derivative). The mass spectrum was recorded in the absence of the lock standard to improve the sensitivity, see the experimental section above for additional details.

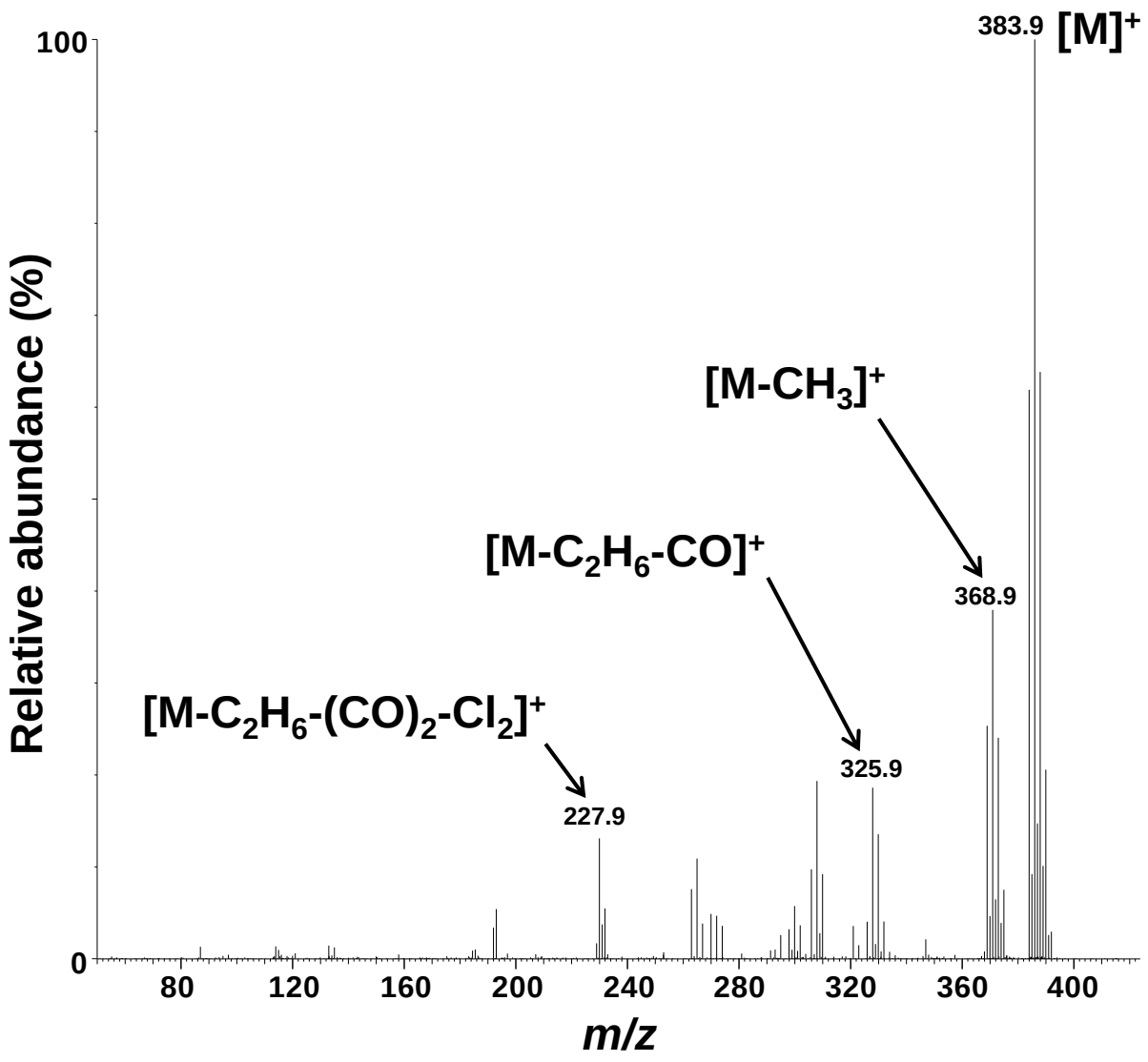

Figure S13. Mass spectrum of M_3-95 (RT 7.08; RRT 1.624), a peak tentatively identified as a dihydroxylated metabolite, formed in incubations of PCB 95 with pooled human liver microsomes. The accurate mass determination of the monoisotopic $[M]^+$ (*m/z* 383.9088 compared to *m/z* 383.9045, calculated for $C_{14}H_9O_2{}^{35}Cl_5$), the isotope pattern of the molecular ion (abundance ratio: 1:1.6:1:0.3 compared to predicted abundance ratio 1:1.6:1:0.3) and the fragmentation pattern are consistent with a dihydroxylated pentachlorobiphenyl (as the corresponding methylated derivative). The mass spectrum was recorded in the absence of the lock standard to improve the sensitivity, see the experimental section above for additional details.

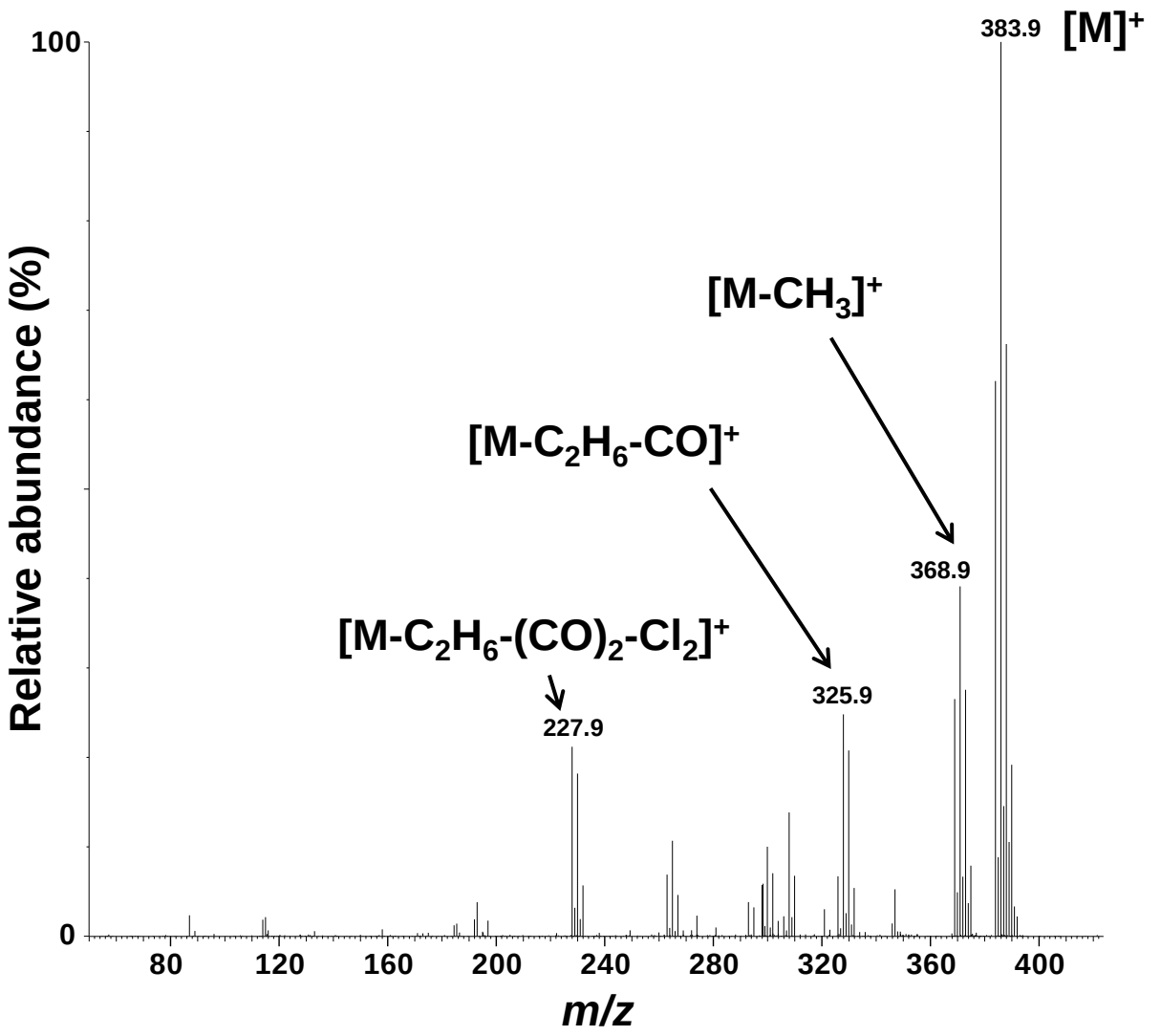

Figure S14. Mass spectrum of 4,5-95 (RT 7.17 min; RRT 1.644) formed in incubations of PCB 95 with pooled human liver microsomes. The accurate mass determination of the monoisotopic $[M]^+$ ((*m/z* 383.9044 compared to *m/z* 383.9045, calculated for $C_{14}H_9O_2{}^{35}Cl_5$), the isotope pattern of the molecular ion (abundance ratio: 1:1.6:1.1:0.3 compared to predicted abundance ratio 1:1.6:1:0.3) and the fragmentation pattern are consistent with a dihydroxylated pentachlorobiphenyl (as the corresponding methylated derivative). The mass spectrum was recorded in the absence of the lock standard to improve the sensitivity, see the experimental section above for additional details.

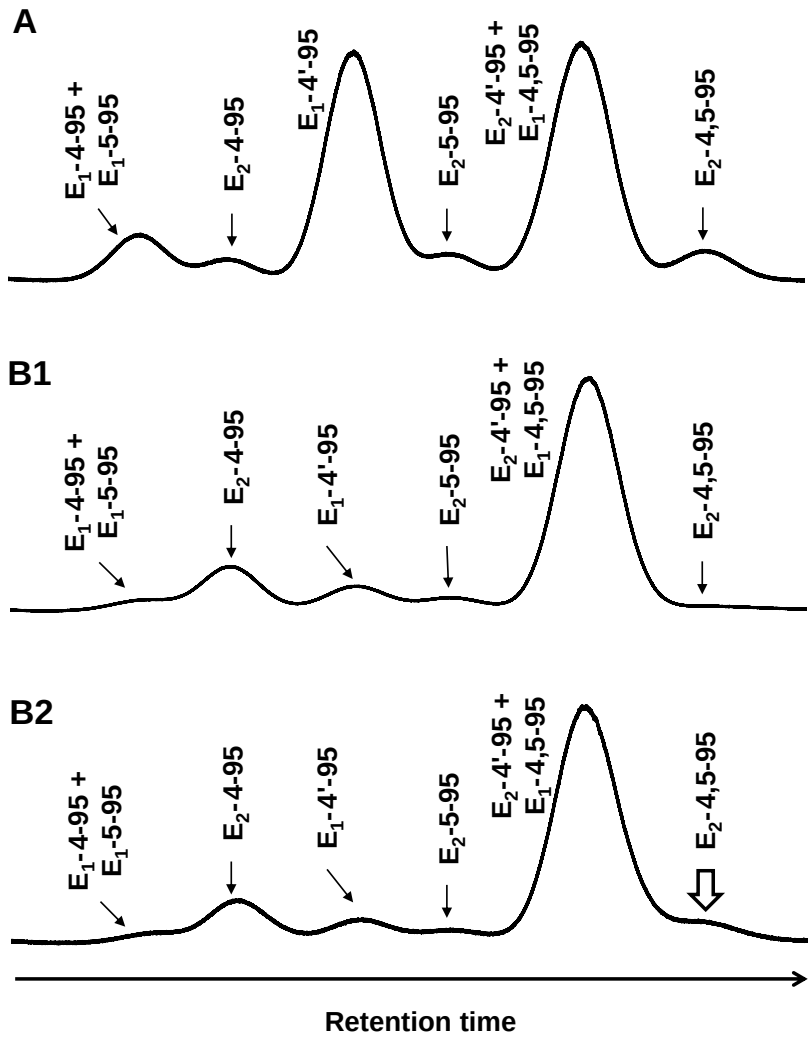

Figure S15. The second eluting atropisomer of 4'-95 (E_2-4'-95) is enriched in a representative extract from an incubation of racemic PCB 95 with HLMs from donor H1, with an apparent EF value of 0.10. (A) Analytical standard containing racemic standards (as methylated derivatives) of 5-95, 4-95, 4'-95 and 4,5-95 in a ratio approximating the metabolite levels reported in Table S1 (1 : 1 : 10 : 0.4 by weight, respectively). (B1) Chromatogram of a representative extract from a microsomal incubation with HLMs from donor H1 (5 μM PCB 95; 120 minute incubation at 37 ºC; 0.5 mg/mL microsomal protein; and 0.5 mM NADPH; see Table S6) showing an atropisomeric enrichment of E_2-4'-95. (B2) Chromatogram of the extract shown in panel B1 spiked with racemic 4,5-95 (0.7 ng) confirming the identification of the E_2-4'-95 atropisomer (broad arrow). Enantioselective analyses were performed on a BDM capillary column as described in the experimental section above.

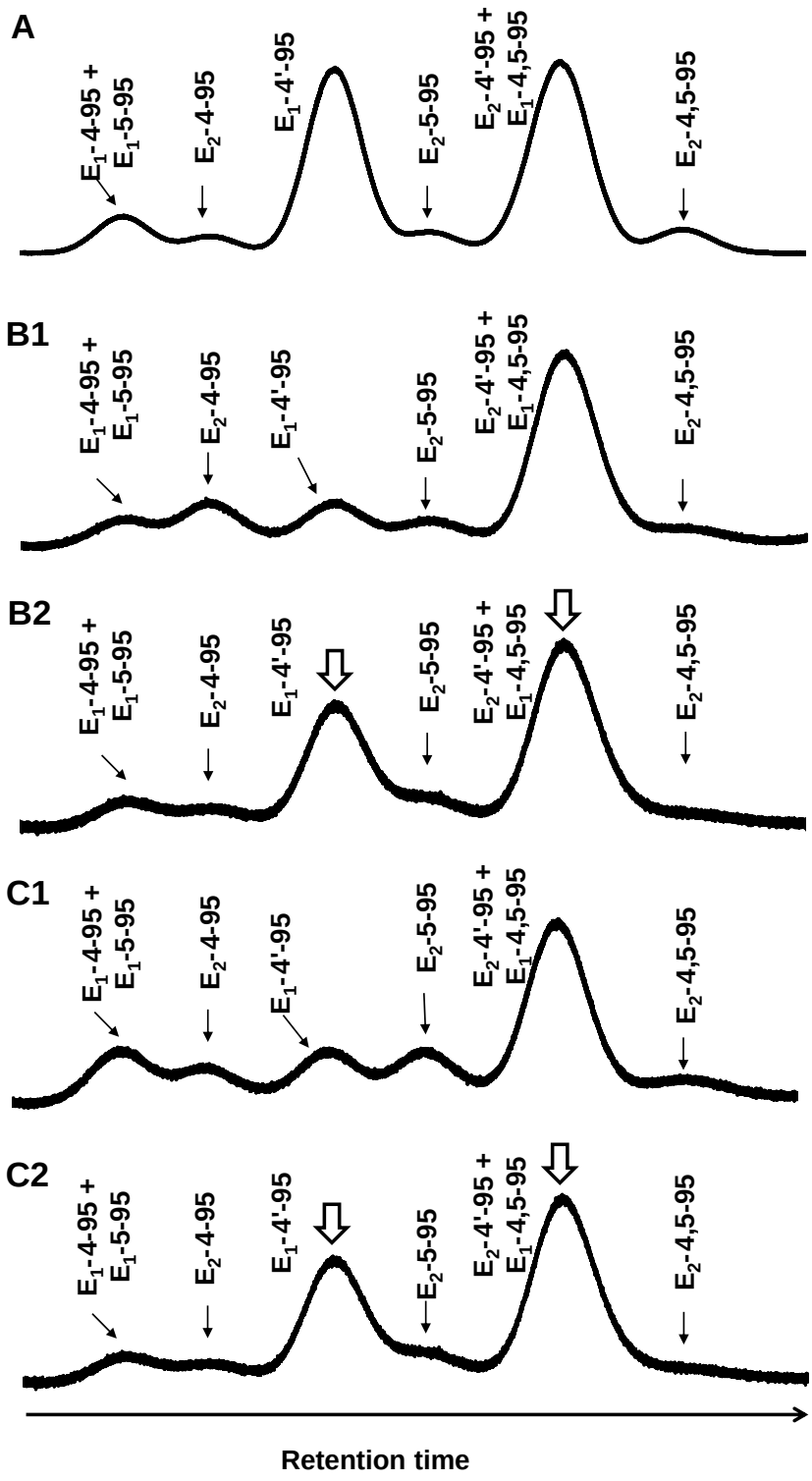

Figure S16. The identification of peaks corresponding to the atropisomers of 4'-95 was verified by spiking selected extracts with racemic 4'-95. (A) Analytical standard containing

racemic standards (as methylated derivatives) of 5-95, 4-95, 4'-95 and 4,5-95 in a ratio approximating the metabolite levels reported in Table S1 (1 : 1 : 10 : 0.4 by weight, respectively; see Figure S15 above). (B1) Chromatogram of a representative extract from a microsomal incubation with HLMs from donor H2 showing an enrichment of E_2-4'-95. (B2) Chromatogram of the extract shown in panel B1 after addition of racemic 4'-95 (4 ng) showing an increase of the two peaks identified as E_1- and E_2-4'-95 based on their retention times. (C1) Chromatogram of a representative extract from a microsomal incubation with HLMs from donor H5 showing an enrichment of E_2-4'-95. (C2) Chromatogram of the extract shown in panel C1 after addition of racemic 4'-95 (4 ng) showing an increase of the two peaks identified as E_1- and E_2-4'-95 based on their retention times. Incubation conditions: 5 μM PCB 95; 120 minute incubation at 37 ºC; 0.5 mg/mL microsomal protein; and 0.5 mM NADPH; see Table S6. Enantioselective analyses were performed on a BDM capillary column as described in the experimental section above.

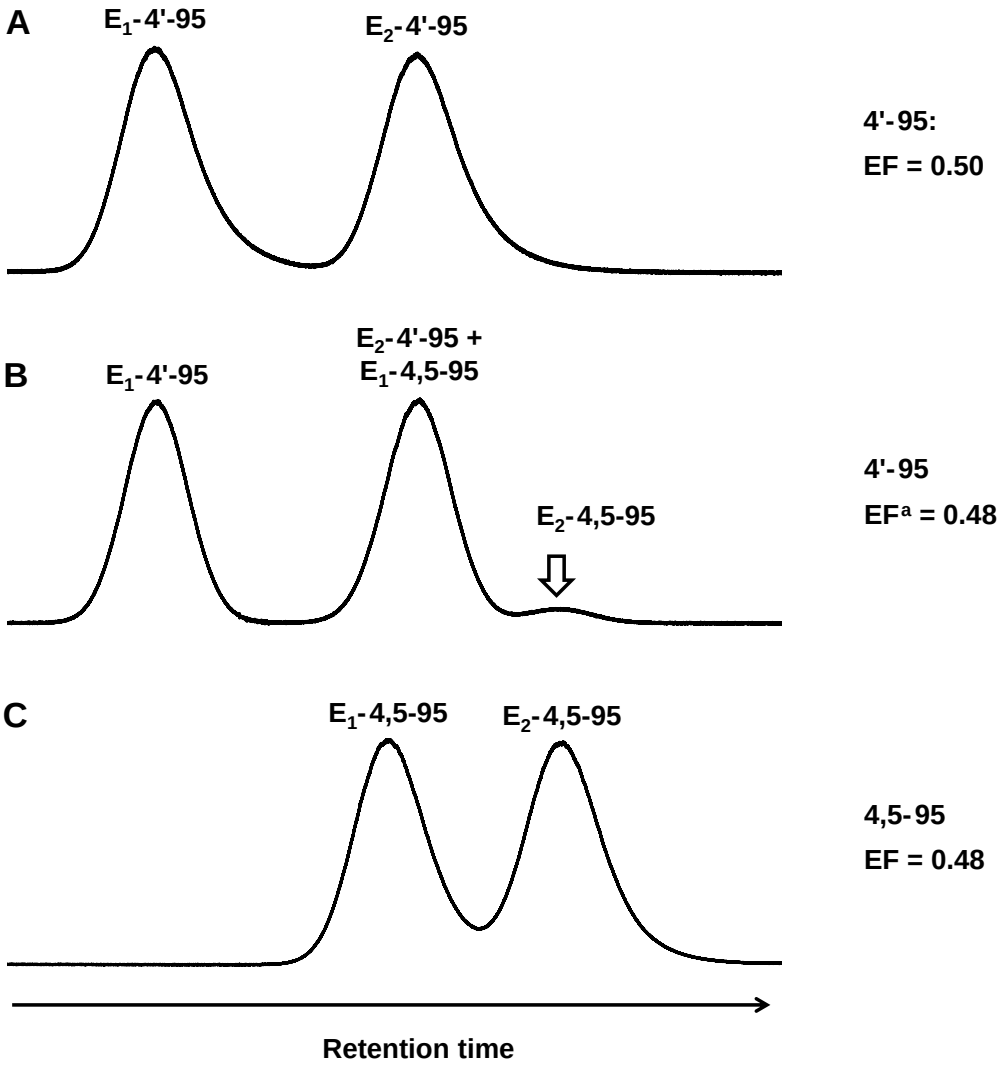

Figure S17. The co-elution of trace amounts of E_1-4,5-95 with E_2-4'-95 only slightly alters the apparent enantiomeric fraction of 4'-95. (A) Racemic 4'-95 standard (50 ng) with an EF value of 0.50, (B) racemic 4'-95 standard (50 ng) spiked with a racemic 4,5-95 standard (1 ng) with an apparent EF value of 0.48, and (C) racemic 4,5-95 standard (50 ng) with an EF value of 0.48. The composition of the spiked sample reflects levels of 4,5-95 that are approximately 1% of the levels of 4'-95 in incubations with HLMs (Table S1) and simulates the effect of the enantiospecific formation of E_1-4,5-95 on the enantiomeric fraction of 4'-95 (i.e., 50 ng of 4'-95 *vs.* 0.5 ng of E_1-4,5-95). Enantioselective analyses were performed on a BDM capillary column as described in the experimental section above. [a] Apparent EF of 4'-95 in the presence of co-eluting E_1-4,5-95 (0.5 ng).

References

1. Kania-Korwel, I., Vyas, S. M.; Song, Y., Lehmler, H.-J. (2008) Gas chromatographic separation of methoxylated polychlorinated biphenyl atropisomers. *J. Chromatogr. 1207*, 146-154.
2. Joshi, S. N., Vyas, S. M., Duffel, M. W., Parkin, S., Lehmler, H.-J. (2011) Synthesis of sterically hindered polychlorinated biphenyl derivatives. *Synthesis 7*, 1045-1054.
3. Ma, C., Zhai, G., Wu, H., Kania-Korwel, I., Lehmler, H. J., Schnoor, J. L. (2016) Identification of a novel hydroxylated metabolite of 2,2',3,5',6-pentachlorobiphenyl formed in whole poplar plants. *Environ. Sci. Pollut. Res. Int. 23*,2089-2098.
4. Wu, X., Pramanik, A., Duffel, M. W., Hrycay, E. G., Bandiera, S. M., Lehmler, H.-J., Kania-Korwel, I. (2011) 2,2',3,3',6,6'-Hexachlorobiphenyl (PCB 136) is enantioselectively oxidized to hydroxylated metabolites by rat liver microsomes. *Chem. Res. Toxicol. 24*, 2249-2257.
5. Kania-Korwel, I., Duffel, M. W., Lehmler, H.-J. (2011) Gas chromatographic analysis with chiral cyclodextrin phases reveals the enantioselective formation of hydroxylated polychlorinated biphenyls by rat liver microsomes. *Environ. Sci. Technol. 45*, 9590-9596.
6. Kania-Korwel, I., Zhao, H., Norstrom, K., Li, X., Hornbuckle, K. C., Lehmler, H.-J. (2008) Simultaneous extraction and clean-up of PCBs and their metabolites from small tissue samples using pressurized liquid extraction. *J. Chromatogr. A 1214*, 37-46.
7. Kania-Korwel, I., Shaikh, N. S., Hornbuckle, K. C., Robertson, L. W., Lehmler, H.-J. (2007) Enantioselective disposition of PCB 136 (2,2',3,3',6,6'-hexachlorobiphenyl) in C57BL/6 mice after oral and intraperitoneal administration. *Chirality 19*, 56-66.
8. Kania-Korwel, I., Hornbuckle, K. C., Peck, A., Ludewig, G., Robertson, L. W., Sulkowski, W. W., Espandiari, P., Gairola, C. G., Lehmler, H.-J. (2005) Congener specific tissue distribution of Aroclor 1254 and a highly chlorinated environmental PCB mixture in rats. *Environ. Sci. Technol.* 39, 3513-3520.
9. EU Commission (2002) Commission Decision EC 2002/657 of 12 August 2002 implementing Council Directive 96/23/EC concerning the performance of analytical methods and the interpretation of results. *Off. J. Eur. Communities: Legis. 221*.
10. Wu, X., Kania-Korwel, I., Chen, H., Stamou, M., Dammanahalli, K. J., Duffel, M., Lein, P. J., Lehmler, H.-J. (2013) Metabolism of 2,2',3,3',6,6'-hexachlorobiphenyl (PCB 136)

atropisomers in tissue slices from phenobarbital or dexamethasone-induced rats is sex-dependent. *Xenobiotica 43*, 933-947.

11. Wu, X. N., Lehmler, H. J. (2016) Effects of thiol antioxidants on the atropselective oxidation of 2,2',3,3',6,6'-hexachlorobiphenyl (PCB 136) by rat liver microsomes. *Environ. Sci. Pollut. Res. Int. 23*, 2081-2088.
12. Asher, B. J., D'Agostino, L. A., Way, J. D., Wong, C. S., Harynuk, J. J. (2009) Comparison of peak integration methods for the determination of enantiomeric fraction in environmental samples. *Chemosphere 75*, 1042-1048.
13. Lupton, S. J., McGarrigle, B. P., Olson, J. R., Wood, T. D., Aga, D. S. (2009) Human liver microsome-mediated metabolism of brominated diphenyl ethers 47, 99, and 153 and identification of their major metabolites. *Chem. Res. Toxicol. 22*, 1802-1809.
14. Wu, X., Kammerer, A., Lehmler, H. J. (2014) Microsomal oxidation of 2,2',3,3',6,6'-hexachlorobiphenyl (PCB 136) results in species-dependent chiral signatures of the hydroxylated metabolites. *Environ. Sci. Technol. 48*, 2436-2444.